Received: 3 August 2022 | Revised: 1 January 2023 | Accepted: 1 March 2023

DOI: 10.1002/ajmg.a.63180

ORIGINAL ARTICLE

AMERICAN JOURNAL OF medical genetics PART A WILEY

An investigation of the etiology and follow-up findings in 35 children with overgrowth syndromes, including biallelic *SUZ12* variant

Aylin Yüksel Ülker[1] | Dilek Uludağ Alkaya[1] | Ahmet Okay Çağlayan[2] | Esra Usluer[1] | Ayça Aykut[3] | Ayça Aslanger[4] | Mehmet Vural[5] | Beyhan Tüysüz[1]

[1]Department of Pediatric Genetics, Cerrahpasa Medical Faculty, Istanbul University-Cerrahpasa, Istanbul, Turkey

[2]Departments of Neurosurgery, Neurobiology and Genetics, Yale School of Medicine, New Haven, Connecticut, USA

[3]Department of Medical Genetics, Faculty of Medicine, Ege University, Izmir, Turkey

[4]Department of Medical Genetics, Bezmialem University, Istanbul, Turkey

[5]Department of Neonatology, Cerrahpasa Medical Faculty, Istanbul University-Cerrahpasa, Istanbul, Turkey

Correspondence
Beyhan Tüysüz, Department of Pediatric Genetics, Istanbul University-Cerrahpasa, Cerrahpasa Medical School, Istanbul, Turkey.
Email: beyhan@istanbul.edu.tr

Funding information
Scientific Research Project Coordination Unit of Istanbul University-Cerrahpasa, Grant/Award Number: TSA-2020-34957

Abstract

Overgrowth-intellectual disability (OGID) syndromes are clinically and genetically heterogeneous group of disorders. The aim of this study was to examine the molecular etiology and long-term follow-up findings of Turkish OGID cohort. Thirty-five children with OGID were included in the study. Single gene sequencing, clinical exome analysis, chromosomal microarray analysis and whole exome sequencing were performed. Five pathogenic copy number variants were detected in the patients; three of them located on chromosome 5q35.2 (encompassing *NSD1*), others on 9q22.3 and 22q13.31. In 19 of 35 patients; we identified pathogenic variants in OGID genes associated with epigenetic regulation, *NSD1* ($n = 15$), *HIST1H1E* ($n = 1$), *SETD1B* ($n = 1$), and SUZ12 ($n = 2$). The pathogenic variants in *PIK3CA* ($n = 2$), *ABCC9* ($n = 1$), *GPC4* ($n = 2$), *FIBP* ($n = 1$), and *TMEM94* ($n = 1$) which had a role in other growth pathways were detected in seven patients. The diagnostic yield was 31/35(88%). Twelve pathogenic variants were novel. The common facial feature of the patients was prominent forehead. The patients with Sotos syndrome were observed to have milder intellectual disability than patients with other OGID syndromes. In conclusion, this study showed, for the first time, that biallelic variants of *SUZ12* caused Imagawa-Matsumoto syndrome, monoallelic variants in *SETDIB* resulted in OGID. Besides expanded the phenotypes of very rare OGID syndromes caused by *FIBP* and *TMEM94*.

KEYWORDS
CMA, intellectual disability, OGID, overgrowth, WES

1 | INTRODUCTION

Generalized overgrowth is defined as height and/or head circumference above 2 standard deviation (*SD*) for age- and sex-matched controls of the population (Baujat et al., 2005). Overgrowth-intellectual disability (OGID) syndromes are diagnosed when excessive growth is accompanied by facial dysmorphism, congenital anomalies, developmental delay (DD)/intellectual disability (ID), behavioral disorders and increased risk of neoplasia (Baujat et al., 2005; Brioude et al., 2019; Neylon et al., 2012). The etiology of OGID syndromes is heterogeneous. The most important mechanism in overgrowth is the disruption of epigenetic regulation; *DNMT3A* (MIM # 602769), *NSD1* (MIM#606681), *HIST1H1E* (MIM#142220), *SETD2* (MIM#612778), *EED* (MIM#605984), *EZH2* (MIM#601573), and *SUZ12* (MIM#

606245) are the genes involved in histone modification, chromatin modeling, or DNA methylation, causing OGID. Sotos syndrome (MIM#117550), caused by *NSD1* mutations, is the most common form of OGID syndromes with an incidence of 1/14,000 live births. Clinical findings are characterized by learning disability and distinctive facial appearance consisted of long face, broad and prominent forehead, sparse frontoparietal hair, and long chin (Tatton-Brown et al., 2019). The *EZH2*, *EED*, and *SUZ12* genes encode proteins that contain core components of polycomb repressive complex 2 (PRC2) that play an essential role in gene silencing. PRC2-related overgrowth syndromes include Weaver syndrome (MIM#277590), Cohen–Gibson syndrome (MIM#617561), and Imagawa-Matsumoto syndrome (MIM #618786), caused by mutations in *EZH2*, *EED*, and *SUZ12*, respectively. These three syndromes have overlapping clinical characteristics such as prenatal and postnatal overgrowth, advanced bone age, musculoskeletal abnormalities, distinctive craniofacial features, and variable intellectual impairment (Cyrus, Burkardt, et al., 2019). Dysregulation of cell cycle is another cause of OGID syndromes. PI3K/AKT/mTOR pathway plays an important role in cell cycle regulation, and *PIK3CA* (MIM#171834) mutations cause *PIK3CA*-related overgrowth spectrum (Burkardt et al., 2019; Edmondson & Kalish, 2015; Kamien et al., 2018; Malan et al., 2010; Tatton-Brown et al., 2017; Tatton-Brown & Weksberg, 2013).

In a recent study, chromosomal microarray (CMA) approach was proposed as the primary test in the diagnosis of the patients with generalized overgrowth without a recognizable phenotype and emphasized that some microdeletion or microduplication syndromes such as 5q35.3 deletion and 15q26 duplication are often associated with overgrowth (Kamien et al., 2018). Next-generation sequencing technology has allowed the identification of novel OGID syndromes, such as disorders caused by biallelic *TMEM94* and *FIBP* mutations (MIM#618306 and MIM#617107), and has led to the identification of other underlying pathophysiological pathways (Akawi et al., 2016; Stephen et al., 2018; Thauvin-Robinet et al., 2016). Although overgrowth syndromes are mostly autosomal dominant inheritance, autosomal recessive inheritance has also been reported, including biallelic mutations in *HERC1*, *DIS3L2*, and *FIBP* (Akawi et al., 2016; Burkardt et al., 2019).

The aim of this study is to investigate the genetic etiology of a Turkish cohort with OGID syndrome, consisted of 35 patients, and to evaluate the long-term clinical features of the patients, and their genotype–phenotype correlation.

2 | METHODS

2.1 | Patients

A total of 35 individuals (25 boys and 10 girls) with overgrowth, DD/ID/autism spectrum disorders and facial dysmorphism were included in the study. Patients with length and/or weight above 2 *SD* at birth were considered as macrosomia. Patients with height and/or head circumference above 2 *SD* for age- and sex-matched controls for Turkish population were also included in the postnatal period. This cohort was selected among the patients followed by one single pediatrics geneticist, during the last 20 years, in a reference center for rare genetic syndromes. Beckwith-Wiedemann syndrome, isolated segmental overgrowth, and metabolic and endocrine disorders were were excluded. Clinical and radiological findings were assessed at diagnosis and in the follow up. Height, weight, and head circumference were measured by a pediatrician, and standard deviation scores (SDS) of anthropometric measurements were obtained. SDS was calculated by using a national pediatric calculator loaded with national standards (https://www. ceddcozum.com). The Denver Developmental Screening Test II (DDST) or the WISC-R were used to assess developmental delay and intellectual disability. Signed informed consent and the permission for the publication of clinical information and the photos of children were obtained from the parents. The Ethics Committee of Cerrahpaşa Medical Faculty at Istanbul University-Cerrahpaşa approved this study (no: 53729, 13.04.2020).

2.2 | Genetic studies and algorithm

Genomic DNA was extracted from peripheral blood cells of the patients and parents using standard techniques. Initially, single gene sequencing or clinical exome analysis was performed in 20 patients clinically diagnosed with known single gene disorders (Figure 1). CMA was performed in 16 patients without a specific clinical diagnosis or without any mutation in gene sequencing. Whole exome sequencing (WES) was performed in 13 patients: 12 patients without pathogenic copy number variations in microarray analysis and one patient who did not undergo CMA since it was compatible with autosomal recessive inheritance. The confirmation of the detected pathogenic variants by WES and segregation analysis in the families were performed by Sanger sequencing.

2.2.1 | Sequencing of *NSD1*, *ABCC9*, and *PIK3CA*

The primers specific for all coding regions, and exon-intron junctions of *NSD1*, *ABCC9*, and *PIK3CA* were designed. After PCR amplification, amplicon-sequencing reactions were performed on Illumina Miseq platform. The data were analyzed by using NextSeq500 (Illumina) system.

2.2.2 | Chromosomal microarray analysis

For detection of copy number variations, microarray studies were performed using CytoScan Optima Array Kit from Affymetrix. The 320 K kit (320,000 probes) has an overall median probe spacing of 13 kb. All procedures were carried out according to the manufacturer's protocol. Genomic positions were based on the UCSC February 2009 human reference sequence (hg19) (NCBI build 37 reference sequence assembly).

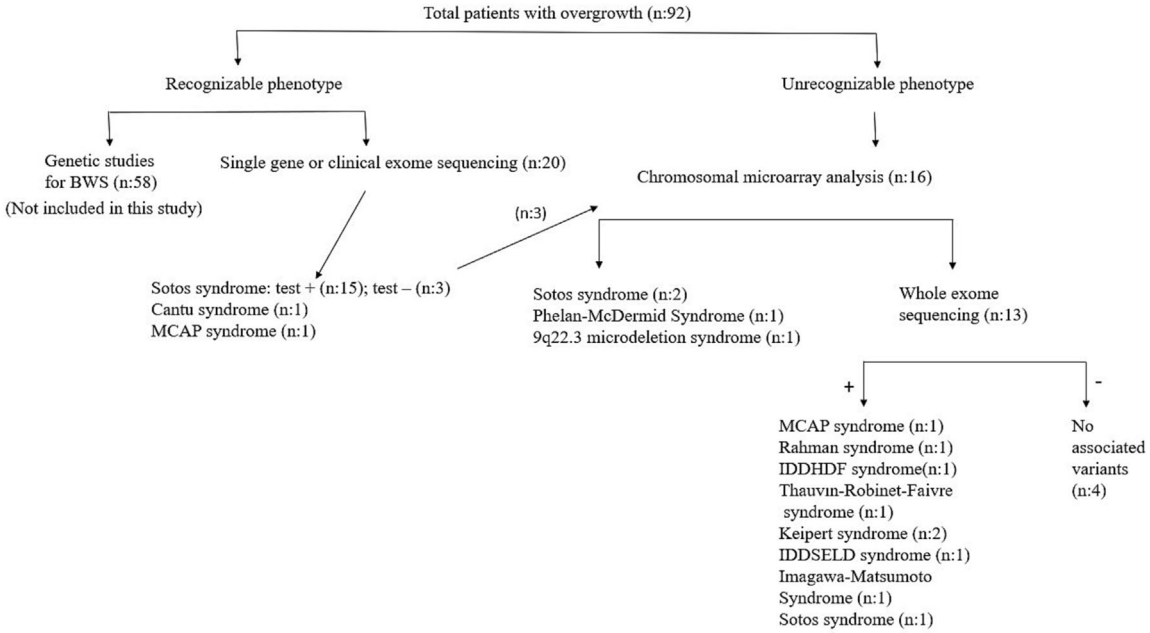

FIGURE 1 Flowchart of the approach used in this study to investigate a group of patients with overgrowth

2.2.3 | Whole exome sequencing

WES was performed on the genomic DNA of the proband and sequenced on the Novoseq platform (Illumina) and CentoXome® MOx Solo (Centogene). Sequences were aligned to the human genome GRCh37/hg19 with BWA-MEM. Variant calls were made with GATK Haplotype Caller and annotated with ANNOVAR. The average sequencing depth was greater than 20 times and the ratio of loci covered was >98%. For variants that had high quality sequence reads (a genotype quality [GQ] ≥20 and MAF $\leq 10^{-2}$ across all samples in gnomAD) were included. The pathogenicity of the variants was determined using the guidelines of the American College of Medical Genetics and Genomics (ACMG; Richards et al., 2015).

2.2.4 | Sanger sequencing

The confirmation of pathogenic variants found by WES analysis and segregation analysis were performed by Sanger sequencing using an ABI PRISM 3500 genetic analyzer (Applied Biosystems, Foster City) and was analyzed with Cutepeaks (https://github.com/labsquare/cutepeaks).

2.3 | Statistical methods

The statistical analyses were performed using IBM Corp. SPSS Statistics® version 21.0. Results were presented as mean ± *SD* or median (min–max value). Mann–Whitney *U* test was performed to compare mean or median values between groups. Categorical values were compared with chi-square and Fisher's exact test. The probability value (*p*-value) less than 0.05, was considered as statistically significant.

3 | RESULTS

The male to female ratio was 2.5. Thirty-one patients were followed up for 1.34–18.8 years and the median follow-up duration was 6.8 years.

3.1 | Molecular studies

Molecular etiology was identified in 31/35 (88%) patients. A 6 Mb microdeletion of the chromosomal region 22q13.31 containing *SHANK3* in one patient and a 4.5 Mb microdeletion in the 9q22.32 domain in another patient were found by CMA. Three patients had a 5q35.2q35.3 microdeletion involving *NSD1*; 1.4 Mb, 1.5 Mb, and 19 Kb (Table 1).

Fourteen variants were identified in the *NSD1*, including five nonsense, four frameshift, two missense, and three splice-site variants (Table 2). Eight of these were novel. A missense c.2176G>A variant was detected by sequencing of the *PIK3CA* from skin sample in a patient who was clinically diagnosed as Megalencephaly-capillary malformation-polymicrogyria syndrome. A missense c.3461G>A variant in *ABCC9* was also found in a boy with Cantu syndrome.

Eight different OGID syndrome related genes were identified in nine patients by WES analysis. Two patients from different families had hemizygous pathogenic variants in *GPC4* inherited from their unaffected mothers (Table 2). Heterozygous de novo variants in the

TABLE 1 Pathogenic copy number variants identified in five patients

Patient number	Genetic test	Copy number variation	Size (genomic position-Hg19)	Coding genes	Main candidate gene	ACMG classification*	Syndrome
1	CMA	9q22.32q22.33 deletion	4.5 Mb (96,893,514_101,449,977) x1	FBP1, C9orf3, FANCC, 5 miRNAs PTCH1, FOXE1, ..., ZNF782) (66 genes)	*PTCH1*	Pathogenic	9q22.3 microdeletion
2	CMA	22q13.31q13.33 deletion	6 Mb (45,099,825_51,197,839) x1	UPK3A, TAFA5, SHANK3, SCO2, CELSR1, ..., PPARA) (94 genes)	*SHANK3*	Pathogenic	Phelan-McDermid
3	CMA	5q35.2q35.3 deletion	1.5 Mb (175,571,150_177,082,381) x1	MIR4281, DDX41, NSD1, F12, SLC34A1, ..., CDHR2 (42 genes)	*NSD1*	Pathogenic	Sotos
4	CMA	5q35.2q35.3 deletion	1.4 Mb (175,750,397_177,136,290)x1	MIR4281, DDX41, NSD1, F12, SLC34A1, ..., CDHR2 (41 genes)	*NSD1*	Pathogenic	Sotos
5	WES	5q35.3 deletion	19Kb (176,718,955_176,738,856)x1	MXD3, RAB24, PRELID1, NSD1 (4 genes)	*NSD1*	Likely Pathogenic	Sotos

Abbreviations: CMA, chromosomal microarray analysis, WES, whole exome sequencing,
[a]The clinical significance of variants was determined per ACMG classification using the Franklin Genoox tool.

PIK3CA, *HIST1H1E*, and *SETD1B* were described in P23, P24, and P29, respectively. P25, P26, and P30 had biallelic variants in *TMEM94*, *FIBP*, and *SUZ12*. Their parents were heterozygous for these variants; the novel biallelic inframe deletion variant in *SUZ12* in P30 was also found in his affected sibling (P31; Table 1). No pathogenic variant was found by WES in four patients.

3.2 | Clinical findings

3.2.1 | The patients diagnosed with CMA

P1 had prenatal-onset overgrowth, DD, cardiovascular and skeletal system abnormalities, and distinct facial features (Table 3, Figure 2e,f) who had a 4.5-Mb microdeletion in the 9q22.3. P2 had a Sotos syndrome-like phenotype, low pain sensitivity, and dystrophic toenails (Figure 2g,h). A 6-Mb microdeletion was detected in the 22q13.31 region containing the *SHANK3* gene, and a Phelan-McDermid syndrome was diagnosed.

3.2.2 | Sotos syndrome

Sotos syndrome was detected in 18 patients (13 boys and five girls). The median age of diagnosis was 3.3 years (range: 0.34–13.9 years). The six patients were diagnosed before the age of one. The mean SDSs of birth length, weight, and head circumference of the patients were 1.42 ± 1.06, 1.21 ± 1.85 and 1.63 ± 1.81, respectively. Patients were followed for a median of 6.84 years (range: 1.34–18.8). While the mean head circumference and height of the patients were 2.16 ± 1.67 and 2.32 ± 1.57 SDS at the first examination, they were 2.62 ± 1.35 and 2.31 ± 1.41 *SD* at the last visit. Fetal macrosomia was detected in eight patients (Table S1). The detailed clinical and craniofacial findings are described in Tables S1 and S2, respectively. The long face, broad forehead, and pointed chin were seen in all patients (Figure 2a–d, Table 3 and Table S2).

While 15 patients had mild developmental delay (DQ = 52–80), P3, P4, and P5 with 5q35 microdeletions had moderate DD (DQ: 48, DQ: 43 and IQ:46). Other clinical findings of the patients were similar in different mutation types were revealed in Table S1. Autistic features were seen in four, attention deficit in four, aggressive behavior in one, and self-mutilation in one patient. Delay of speech were observed in 13 patients (72%). Infantile hypotonia was detected in seven cases. Seizures were seen in 44% of the patients.

Advanced bone age was found in 13 (72%), delayed bone age also was observed in two patients. Cardiac anomalies were detected in seven patients (39%). Likewise, genitourinary abnormalities were noted in seven of them (39%). No tumors were detected in the patients during their follow up (mean 6.84 years).

3.2.3 | Cantu syndrome

Cantu syndrome was clinically diagnosed in P21 with prenatal overgrowth, prominent facial appearance, hypertrichosis, hypertrophic

TABLE 2 Pathogenic variants identified in 26 patients by gene sequencing or whole exome sequencing (WES)

Patient number	Genetic test	Gene	Mutation	Protein change (transcript ID)	Zygosity	Novel/known	Location	Mutation type	ACMG classification	OMIM number/ phenotype name
6	Gene sequencing	*NSD1*	c.1810C>T	p. Arg604Ter (NM_022455.5)	Heterozygous	Known	Exon 5	Nonsense	Pathogenic (PVS1, PM2, PP5)	117,550/Sotos syndrome
7	Gene sequencing	*NSD1*	c.1831C>T	p. Arg611Ter (NM_022455.5)	Heterozygous	Known	Exon 5	Nonsense	Pathogenic (PVS1, PM2,PP5)	117,550/Sotos syndrome
8	Gene sequencing	*NSD1*	c.2014_2018del	p. Thr672GlufsTer9 (NM_022455.5)	Heterozygous	Novel	Exon 5	Frameshift	Pathogenic (PVS1, PM2, PP5)	117,550/Sotos syndrome
9	Gene sequencing	*NSD1*	c.2148del	p. Lys717ArgfsTer17 (NM_022455.5)	Heterozygous	Novel	Exon 5	Frameshift	Likely pathogenic (PVS1, PM2)	117,550/Sotos syndrome
10	Gene sequencing	*NSD1*	c.2905_2908del	p. Gly969MetfsTer70 (NM_022455.5)	Heterozygous	Novel	Exon 5	Frameshift	Likely pathogenic (PVS1, PM2)	117,550/Sotos syndrome
11	Gene sequencing	*NSD1*	c.3292dup	p. Thr1098AsnfsTer3 (NM_022455.5)	Heterozygous	Novel	Exon 5	Frameshift	Likely pathogenic (PVS1, PM2)	117,550/Sotos syndrome
12	Gene sequencing	*NSD1*	c.3610C>T	p. Arg1204Ter (NM_172349.2)	Heterozygous	Known	Exon 11	Nonsense	Pathogenic (PVS1, PP5, PM2)	117,550/Sotos syndrome
13	Gene sequencing	*NSD1*	c.4660G>T	p. Glu1554Ter (NM_022455.5)	Heterozygous	Novel	Exon 12	Nonsense	Likely pathogenic (PVS1, PM2)	117,550/Sotos syndrome
14	Gene sequencing	*NSD1*	c.5098C>T	p. Arg1700Ter (NM_022455.5)	Heterozygous	Known	Exon 14	Nonsense	Pathogenic (PVS1, PM2, PP5)	117,550/Sotos syndrome
15	Gene sequencing	*NSD1*	c.5304-2A>C	(NM_022455.5)	Heterozygous	Novel	Intron 15	Splicing	Likely pathogenic (PVS1, PM2)	117,550/Sotos syndrome
16	Gene sequencing	*NSD1*	c.5622+1G>A	(NM_022455.5)	Heterozygous	Novel	Intron 17	Splicing	Likely pathogenic (PVS1, PM2)	117,550/Sotos syndrome
17	Gene sequencing	*NSD1*	c.5737A>C	p. Asn1913 His (NM_022455.5)	Heterozygous	Known	Exon 18	Missense	Likely pathogenic (PVS1, PP2)	117,550/Sotos syndrome
18	Gene sequencing	*NSD1*	c.5951G>A	p. Arg1984Gln (NM_022455.5)	Heterozygous	Known	Exon 19	Missense	Pathogenic (PM1, PP2, PM2, PM5, PP3, PP5)	117,550/Sotos syndrome
19	Gene sequencing	*NSD1*	c.6151+2T>A	(NM_022455.4)	Heterozygous	Novel	Intron 20	Splicing	Likely pathogenic (PVS1, PM2)	117,550/Sotos syndrome
20	Gene sequencing	*NSD1*	c.6151+2T>A	(NM_022455.4)	Heterozygous	Novel	Intron 20	Splicing	Likely pathogenic (PVS1, PM2)	117,550/Sotos syndrome
21	Gene sequencing	*ABCC9*	c.3461G>A	p. Arg1154Gln (NM_020297.4)	Heterozygous	Known	Exon 29	Missense	Pathogenic (PM2, PM5, PP3, PP2, PP5)	239,850/Cantu syndrome
22	Gene sequencing	*PIK3CA*	c.2176G>A	p. Glu726Lys (NM_006218.4)	Heterozygous Somatic	Known	Exon 14	Missense	Pathogenic (PS4, PS2, PM1, PP2, PM2, PM5, PP5)	602,501/ Megalencephaly-capillary malformation-polymicrogyria syndrome; MCAP

TABLE 2 (Continued)

Patient number	Genetic test	Gene	Mutation	Protein change (transcript ID)	Zygosity	Novel/known	Location	Mutation type	ACMG classification	OMIM number/ phenotype name
23	WES	*PIK3CA*	c.1133G>A	p. Cys378Tyr (NM_006218.4)	Heterozygous	Known	Exon 6	Missense	Pathogenic (PP5, PM2, PP3, PM5, PM1, PP2)	602,501/ Megalencephaly-capillary malformation-polymicrogyria syndrome; MCAP
24	WES	*HIST1H1E*	c.441dupC	p. Lys148GlnfsTer48 (NM_005321.3)	Heterozygous	Known	Exon 1	Frameshift	Pathogenic (PVS1, PM2, PP5)	617,537/Rahman syndrome
25	WES	*TMEM94*	c.3998+5G>A	(NM_014738.6)	Homozygous	Known	Intron 31	Splicing	Likely pathogenic (PP3, PM2, PP5)	618,316/ Intellectual Developmental Disorder with Cardiac defects and Dysmorphic Facies, IDDHDF
26	WES	*FIBP*	c.412-3_415dupCAGTTTG	p. Asp139AlafsTer3 (NM_004214)	Homozygous	Novel	Exon 4	Nonsense	Likely pathogenic (PVS1, PM2)	617,107/Thauvin-Robinet-Faivre syndrome
27	WES	*GPC4*	c.246_252delTTTCAAA	p. Asp82GlufsTer37 (NM_001448.3)	Hemizygous	Novel	Exon 2	Nonsense	Likely pathogenic (PVS1, PM2)	301,026/Keipert syndrome
28	WES	*GPC4*	c.1480del	p. Ser494ValfsTer93 (NM_001448.3)	Hemizygous	Novel	Exon 9	Frameshift	Likely pathogenic (PVS1, PM2)	301,026/Keipert syndrome
29	WES	*SETD1B*	c.5842G>A	p. Glu1948Lys (NM_001353345.2)	Heterozygous	Known	Exon 17	Missense	Likely pathogenic (PS3, PM1, PP5, PM2)	619,000/ Intellectual developmental disorder with seizures and language delay, IDDSELD
30/31	WES	*SUZ12*	c.1239_1241delCAA	p. Asn437del (NM_015355.4)	Homozygous	Novel	Exon 12	In frame deletion	Uncertain Significance (PM2,PM4)	618,786/Imagava-Matsumoto syndrome

TABLE 3 Clinical features of 31 patients with established molecular diagnosis.

		Other overgrowth syndromes															
Diagnoses/ Patient number	Sotos syndrome (n:18)	9q22.3 micro-deletion syndrome (P1)	Phelan-McDermid syndrome (P2)	Cantu syndrome (P21)	Megalencephaly-capillary malformation-polymicrogyria syndrome (P22)	(P23)	Rahman syndrome (P24)	IDDCDF syndrome (P25)	Thauvin-Robinet-Faivre syndrome (P26)	Keipert syndrome (P27)	(P28)	IDDSELD syndrome (P29)	Imagava-Matsumoto syndrome (P30)	(P31)	Total	Overall (n:31)	P value**
Gender	F/M:5/13	F	M	M	F	F	M	M	M	M	M	M	M	M	F/M:3/10	8F/23M	
Consanguineous	7/18	+	-	-	-	-	+	+	+	-	+	-	+	+	7/13	14/31	
Age at first visit (year)	3.3 (median)	0.3	1.0	1.8	1.2	0.6	2.7	2.2	0.5	2.8	1.3	0.4	5.8	NA	1.25 (median)	1.5 (median)	0.17
Birth HC (SDS)	1.63 ± 1.81 (mean)	2.5	1.7	NA	4.5	5.0	NA	2.3	NA	NA	NA	NA	NA	NA	3.2 ± 1.5 (mean)	2.3 ± 1.8 (mean)	0.08
Birth lenght (SDS)	1.42 ± 1.06 (mean)	3.1	0.5	1.9	1.2	3.0	NA	3.5	1.9	NA	NA	0.3	0.2	NA	1.7 ± 1.3 (mean)	1.5 ± 1.1 (mean)	0.44
Birth weight (SDS)	1.21 ± 1.85 (mean)	2.2	0.1	3.4	1.6	3.2	4.3	2.9	2.6	1.4	-0.5	-0.5	3.9	NA	2.1 ± 1.7 (mean)	1.6 ± 1.8 (mean)	0.23
HC (SDS) at first visit	2.16 ± 1.67 (mean)	2.5	2.6	1.9	5	4.2	1	2.3	2.3	0.06	0.4	2.7	0.9	NA	2.2 ± 1.5 (mean)	2.2 ± 1.6 (mean)	0.75
Height (SDS) at first visit	2.32 ± 1.57 (mean)	2.9	4.2	0	-0.01	1.2	-0.5	2.1	1.2	0.7	-2	1.8	1.7	NA	1.1 ± 1.6 (mean)	1.8 ± 1.7 (mean)	0.06
Weight (SDS) at first visit	1.43 ± 1.07 (mean)	1.3	1.5	-0.1	0.9	1.1	2.2	1.6	1.3	2.3	-2.7	1.4	-0.08	NA	0.9 ± 1.3 (mean)	1.2 ± 1.2 (mean)	0.41
Follow-up duration (year)	6.8 (median)	3.6	1.8	NA	NA	9.8	16.0	5.6	17.9	1.8	2.8	11.4	7.9	NA	5.6 (median)	6.8 (median)	0.69
Age (year) at last visit	9.5 (median)	3.9	2.9	2.3	NA	10.4	18.7	7.7	18.4	4.6	4.0	11.8	13.7	NA	7.7 (median)	9.22 (median)	0.52
HC (SDS) at last visit	2.62 ± 1.35 (mean)	1.4	2.9	0.9	NA	5.2	2	3.3	2.2	1.7	-0.07	3.0	2.0	NA	2.2 ± 1.4 (mean)	2.5 ± 1.3 (mean)	0.44
Height (SDS) at last visit	2.31 ± 1.41 (mean)	2.3	3.2	-0.9	NA	1.3	0.7	4.1	2.1	1.9	-2.8	3.3	2.5	NA	1.6 ± 1.9 (mean)	2.0 ± 1.7 (mean)	0.44
Weight (SDS) at last visit	1.39 ± 1.38 (mean)	0.04	0.7	0.9	NA	0.1	2.5	3.7	0.1	2.5	-1.7	2.5	0.71	NA	1.1 ± 1.5 (mean)	1.3 ± 1.4 (mean)	0.42
Craniofacial features																	
Triangular face	-	+	+	-	-	+	-	-	+	-	-	-	+	+	6/13	6/31	0.002
Flat face	-	-	-	-	-	-	-	-	-	+	+	-	-	-	2/13	2/31	0.16
Long-narrow face	18/18	+	+	-	+	+	+	+	-	-	-	+	-	-	7/13	25/31	0.002
Coarse Face	-	+	-	+	-	-	+	+	-	-	-	-	-	-	3/13	4/31	0.023
Hıgh-Broad forehead/	18/18	+	+	-	+	+	+	-	+	+	+	-	+	+	10/13	28/31	0.06
Frontal bossing	11/18	+	-	-	+	+	+	-	-	-	-	-	-	-	4/13	15/31	0.09
Prominent metopic suture	-	-	-	-	-	-	+	+	-	-	-	-	+	+	4/13	4/31	0.02

TABLE 3 (Continued)

Diagnoses/ Patient number	Sotos syndrome (n:18)	Other overgrowth syndromes													Total	Overall (n:31)	P value**
		9q22.3 micro-deletion syndrome (P1)	Phelan-McDermid syndrome (P2)	Cantu syndrome (P21)	Megalencephaly-capillary malformation-polymicrogyria syndrome (P22)	(P23)	Rahman syndrome (P24)	IDDCDF syndrome (P25)	Thauvin-Robinet-Faivre syndrome (P26)	Keipert syndrome (P27)	(P28)	IDDSELD syndrome (P29)	Imagava-Matsumoto syndrome (P30)	(P31)			
Mild downslanting palpebral fissures	6/18	+	+	-	-	-	-	-	+	-	-	-	+	+	5/13	11/31	1.00
Sparse hair/	12/18	-	+	-	-	-	+	-	-	+	+	-	+	+	6/13	18/31	0.25
Sparse eyebrows	12/18	+	+	-	+	-	+	+	-	+	+	-	+	+	9/13	21/31	1.00
Hypertelorism	14/18	+	+	+	+	+	+	+	+	+	+	-	+	+	12/13	26/31	0.36
Epicanthal fold	3/18	+	+	+	-	-	+	+	+	-	-	-	+	+	8/13	11/31	0.02
Broad nasal bridge	-	+	-	+	+	-	+	+	+	-	-	-	-	+	7/13	7/31	0.001
Small nose	15/18	+	-	+	+	+	-	+	+	+	+	-	-	-	8/13	23/31	0.22
Philtrum	N	long	N	N	long	N	N	N	N	short	short	long	N	N			
High-arched palate	13/18	+	-	-	+	-	-	-	+	-	+	-	-	-	4/13	17/31	0.02
Micrognathia	3/18	-	-	-	+	+	-	+	-	+	+	-	-	+	6/13	9/31	0.11
Pointed chin	18/18	-	+	-	-	-	-	-	+	-	-	-	-	-	2/13	20/31	0.00
Strabismus	6/18	-	+	-	-	-	-	+	-	+	-	-	-	-	3/13	9/31	0.69
Others	Malar flushing (9/18)	Sagging cheeks		Thick lips, hypertrichosis, long curly eyelashes, antevert nares	Upslanted and short palpebral fissure		Deep set eyes, high nasal bridge, full cheek	Large pinnae, eversion of lateral eylids,	Thick and arched eyebrows,	Full cheek, wide mounth, antevert nares	wide mounth, antevert nares	Bifrontal narrowing, smooth phıltrum, high nasal bridge	Beaked nose, maxillar hypoplasia, high nasal bridge				
Neurological features																	
Motor reterdation	17/18	+	+	-	+	+	+	+	+	+	+	+	+	NA	11/13	28/31	0.3
Delay in speech	13/18	+	+	-	-	+	+	+	+	+	+	+	+	NA	10/13	23/31	1.0
IQ/DQ (last examination)	69 (median)	DQ:44	DQ:43	DQ:90	DQ:85	DQ:50	DQ:43	IQ:40	IQ:71	DQ:57	DQ:50	DQ:54	DQ:30	NA	50 (median)	59 (median)	0.09
Behaviour disorder	9/18	-	+	-	-	-	-	-	-	+	-	-	-	NA	2/13	11/31	0.06
Seizures	8/18	+	-	-	-	+	-	-	-	+	-	+	-	NA	4/13	12/31	0.70
MRI abnormalities																	
Thinning of corpus callosum	9/18	+	+	-	-	-	-	-	-	-	-	+	-	NA	3/13	12/31	0.12
Ventriculomegaly	9/18	-	+	-	-	+	-	+	-	+	+	-	+	NA	6/13	15/31	1.00
Skeletal system features																	
Advanced bone age	13/18	-	-	-	NA	-	+	+	-	+	-	-	+	NA	4/13	17/31	0.02
Scoliosis/kyphosis	12/18	+	-	-	-	+	-	+	-	-	-	-	+	NA	4/13	16/31	0.05
	1/18	-	+	-	-	-	-	-	-	-	-	-	-		1/13	2/31	1.0
Coxa valga	9/18	-	-	+	-	+	-	-	+	-	-	-	+	NA	4/13	13/31	0.48

(Continues)

TABLE 3 (Continued)

Diagnoses/ Patient number	Sotos syndrome (n:18)	Other overgrowth syndromes																		Overall (n:31)	P value**
		9q22.3 micro-deletion syndrome (P1)	Phelan-McDermid syndrome (P2)	Cantu syndrome (P21)	Megalencephaly-capillary malformation-polymicrogyria syndrome		Rahman syndrome (P24)	IDDCDF syndrome (P25)	Thauvin-Robinet-Faivre syndrome (P26)	Keipert syndrome		IDDSELD syndrome (P29)	Imagava-Matsumoto syndrome							
					(P22)	(P23)				(P27)	(P28)		(P30)	(P31)	Total					
Pes planus	8/18	-	-	+	-	-	-	-	-	-	-	+	-	NA	2/13	10/31	0.12				
Large hands and/or feet	15/18	-	-	-	-	-	+	+	+	-	-	-	-	NA	3/13	18/31	0.001				
Cardiovascular abnormalities (total)	7/18	+	+	+	-	+	-	+	+	+	-	-	-	NA	7/13	14/31	0.40				
Genitourinary abnormalities	7/18	+	+	-	-	-	+	-	-	-	+	-	+	NA	5/13	12/31	0.98				

Note: Intellectual developmental disorder with cardiac defects and dysmorphic facies; IDDCDF syndrome (OMIM* 618163), Intellectual developmental disorder with seizures and language delay; IDDSELD (OMIM* 611055).
Abbreviations: F, Female; HC, head circumference; M, male; N, normal; NA, not available; SDS, standard deviation scores.
[a]Shows the statistical analysis of between Sotos syndrome and other OGID groups.

cardiomyopathy, umbilical hernia, and skeletal findings, including narrow thorax, broad ribs, ovoid vertebral bodies, hypoplastic acetabuli, coxa valga, and hallux valgus (Table 3).

3.2.4 | Megalencephaly-capillary malformation-polymicrogyria syndrome

Megalencephaly-capillary malformation-polymicrogyria syndrome (MCAP) was clinically diagnosed in P22, who exhibited severe macrocephaly since birth, facial dysmorphism, capillary hemangioma, and lateralized overgrowth (Table 3).

3.2.5 | The patients diagnosed with WES

Heterozygous mutation in *PIK3CA*, *HIST1H1E*, and *SETD1B* caused MCAP syndrome in P23, Rahman syndrome in P24 (Figure 2i,j) and Intellectual developmental disorder with seizures and language delay (IDDSELD) in P29 (Figure 2k,l), respectively. Hemizygous pathogenic variants in *GPC4* caused Keipert syndrome in P27 and in P28 (Figure 2m,n). All of them had dysmorphic craniofacial features, varying degrees of developmental delay and intellectual disability with cranial MRI abnormalities (Table 3). P25 with Intellectual developmental disorder with cardiac defects and dysmorphic facies (IDDCDF) syndrome (Figure 2o,p) had prenatal-onset overgrowth, dysmorphic facial features, advanced bone age, scoliosis, pectus excavatum, and inguinal hernia. P26 with Thauvin-Robinet Faivre syndrome (Figure 2q,r) presented at the age of 6.5 months with macrocephaly, DD, pectus excavatum, inverted nipples, umbilical hernia, and coxa valga (Table 3). Tall stature developed over time in childhood.

The sibling (P30 and P31) with Imagawa-Matsumoto syndrome had a round face, prominent forehead, hypertelorism, epicanthal fold, micrognathia, and full cheeks in infancy (Figure 3a,f–h). However, an elongated triangular face and a beaked nose developed over time in Patient 30 (Figure 3a–c). They also had skeletal system findings such as elbows/knees contractures, elbow dislocation, camptodactyly, coxa valga and advanced bone age (Figure 3d,e,j). The most severe developmental delay was observed in P30; he sat independently at about 5 years of age, could never walk independently, and could speak only two words.

3.3 | Four patients without molecular diagnosis

P32 had overgrowth, ID, epilepsy, autistic and aggressive behavior, and facial dysmorphism (Figure 4a,b). His parents were first cousin and there were many individuals with ID in his family whose growth patterns were not known. P33 had infantile hypotonia, overgrowth, ID, pectus excavatum, hypermobile elbows, camptodactyly, partially webbed fingers, ventriculomegaly and corpus callosum agenesis, ureteropelvic junction stenosis, and dysmorphic facial features (Figure 4c). P34 had prenatal overgrowth, DD, Weaver syndrome-like

FIGURE 2 Facial photographs of the patients with Sotos syndrome and other OGID syndromes. *First row*: photographs of patients with Sotos syndrome at different ages (a–d), and patient 1 with 9q22.3 microdeletion syndrome (e, f). Patient 3 at the age of 6.5 months (a), patient 10 at the age of 4 years (b), patient 9 at the age of 4 and 19 years (c, d). The distinctive facial appearance was seen in patients with Sotos syndrome; long face, broad forehead, hypertelorism, mild down slanting palpebral fissures, and pointed chin (a–d); sparse hair in the frontoparietal area, small nose and nasal tip (a, b). Note that a long and narrow face in childhood enlarges over time (c, d). Patient 1 with 9q22.3 microdeletion syndrome has coarse face, high broad forehead, frontal bossing, hypertelorism, epicanthal folds, long philtrum, and sagging cheeks (e, f). *Second row*: Patient 2 with Phelan-McDermid syndrome at the age of 2.5 years (g, h); patient 24 with Rahman syndrome at the age of 6 years (i), and 18 years (j); patient 29 with IDDSELD syndrome at the age of 1.5 years (k), and 11.5 years (l). Patient 2 is exhibiting Sotos-like phenotype with sparse hair, long face, broad forehead, mild downslanting palpebral fissure, and hypertelorism (g, h). Patient 24 had full cheeks, high frontal hairline, bitemporal narrowing, deep-set eyes, hypertelorism, and prominent metopic suture (i, j). Patient 29 had bifrontal narrowing, smooth philtrum (l), and also elongation of the face with age are notable (k, l). *Third row*: Patients 27 and 28 with Keipert syndrome at the age of 4.5 years (m) and 2 years (n), respectively; patient 25 with IDDCDF syndrome at the age of 2 years (o), and 8 years (p), patient 26 with Thauvin-Robinet-Faivre syndrome at the age of 3.5 years (q), and 18 years (r). Patients 27 and 28 had flat face, high-broad forehead, hypertelorism, small nose, short philtrum, antevert nares, wide mouth, and micrognatia (m, n). Patient 25 has long and coarse face, prominent metopic suture, hypertelorism, epicanthal folds, large pinnae, short palpebral fissure, and micrognatia (o, p). Patient 26 had triangular face, hypertelorism (q, r) also deep-set eyes and thick eyebrows became evident with age (q, r)

facial features, kyphoscoliosis, joint contractures (elbows, knees), advanced bone age, and a high pitched voice (Figure 4d,e). After the age of 6.5, she became unable to walk and dependent on a wheelchair. P35 had the Sotos syndrome-like phenotype (Figure 4f).

4 | DISCUSSION

Although the new OGID syndromes have been described in recent years, the molecular etiology is still unknown in approximately 50% (Tatton-Brown et al., 2017). In a study with overgrowth syndrome, 42% were diagnosed with exome sequencing and CMA; Of these, 53% had mutations in genes involved in epigenetic regulation (Moirangthem et al., 2021). The diagnostic yield of WES, targeted gene sequencing and CMA in our OGID syndrome cohort was 88%; pathogenic variants in genes were associated with epigenetic regulation in 22/31 patients (70.9%), of which 81.8% were Sotos syndrome. The high diagnosis rate in our cohort can be explained by the clinically easily recognizable Sotos syndrome, which constitutes more than half of all our patients.

Recently, overgrowth syndromes have been classified into three groups according to the underlying mechanisms; (1) Inborn errors of epigenetic regulation and associated transcription factors; (2) The PI3K-AKT–MTOR signaling pathway; (3) Genes associated with other functional pathways (Burkardt et al., 2019). We discussed the results of our

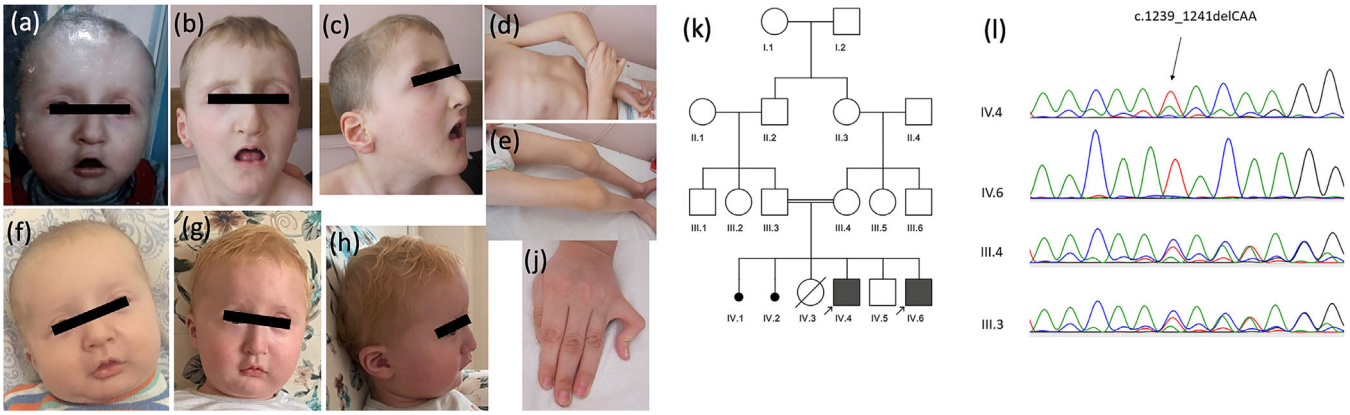

FIGURE 3 Photographs of Patients 30 and 31 (two siblings) with a biallelic mutation in *SUZ12*. Patient 30 at the age of 4 months (a), and 7 years (b, c); patient 31 at the age of 3 months (f), and 1 year (g, h). Two siblings had a round face, prominent forehead, hypertelorism, epicanthal fold, micrognathia, and full cheeks in their infancy period (a, f), and an elongated face and beak-shaped nose developed in patient 30 over time (b, c). Contractures in the elbow and knee (d, e), and camptodactyly (j) were observed in Patient 30 at the age of 7 years. Pedigree of the family (k), and Sanger sequencing and segregation analysis (l) of the *SUZ12* variant. Chromatogram was arranged from top to bottom as proband, affected sibling, mother, and father, probands were homozygous and parents were heterozygous for the c.1239_1241delCAA *SUZ12* variant

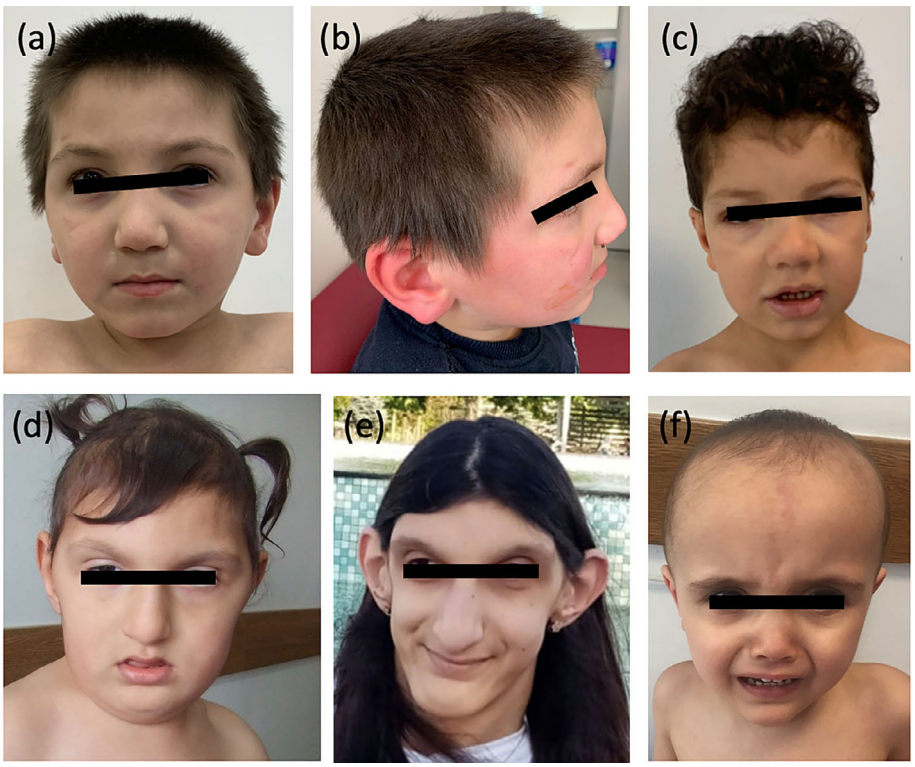

FIGURE 4 Photographs of patients without a molecular diagnosis. *First row*: Patient 32, a 4.5-year-old boy, had a flat face, thin eyebrows, long palpebral fissures, hypertelorism, high nasal bridge, thick nasal alae, and wide earlobes (a, b). Patient 33 had hypertelorism, low nasal bridge, and thick nasal alae at the age of 4.5 years (c). *Second row*: patient 34 at age of 4 years (d), and 13 years (e); she had coarse and long face, downslanting palpebral fissures, hypertelorism, and large ears. The prominent ears, elongation of the face and chin with age are notable (e). Patient 35 had triangular face, frontoparietal sparse hair, frontal bossing, broad forehead, capillary hemangioma at the forehead, and pointed chin at the age of 3 years (f)

cohort in three groups as microdeletion syndromes, disorders in epigenetic mechanisms, and disorders in genes involved in other pathways.

4.1 | Microdeletion syndromes

Prenatal-onset overgrowth was reported in 20% of patients with 9q22.3 microdeletion syndrome, characterized by developmental delay and basal cell nevus (Gorlin) syndrome symptoms (Muller et al., 2012). Among the 9q22.3 microdeletion patients with overgrowth and/or macrosomia, a 550 Kb region encompassing *PTCH1*, *C9orf3*, *FANCC*, and five miRNAs has been reported to be the most frequently deleted common region (Yamada et al., 2020). This region was also deleted in our Patient 1 with 9q22.3 microdeletion syndrome. At the last examination, she was 3.9 years old and had no signs of Gorlin syndrome.

Phelan-McDermid syndrome is a neurodevelopmental disorder caused by *SHANK3* deletions or mutations on 22q12.31. A recent study reported that 31.9% of patients with Phelan-McDermid

syndrome had overgrowth and the patients with a large deletion 22q encompassing with *SHANK3* had a higher overgrowth rate than those with an intragenic variant (Nevado et al., 2022). Our patient with this syndrome had a Sotos syndrome-like facial features such as long face, high-broad forehead, sparse hair, hypertelorism, and pointed chin.

In addition, 1.5 and 1.4 Mb microdeletions covering *NSD1* in the 5q35 domain were detected by CMA in two patients with Sotos syndrome, and 19Kb deletion was by WES in one.

4.2 | Syndromes due to defect in epigenetic regulation

4.2.1 | Sotos syndrome

Sotos syndrome resulting from the 5q35 microdeletion is rare outside the Japanese population and accounts for approximately 10% of all affected individuals (De Boer et al., 2004; Tatton-Brown et al., 2005; Tony et al., 2005). We found pathogenic variants in 18 patients in *NSD1* (Table 2); 5q35 microdeletion was found in three patients (17%), and 15 (83%) intragenic mutations in *NSD1*, all of them de novo. The protein truncating mutations were found to be scattered throughout the gene with the majority in exons 5 (5/12; 42%), whereas the two missense mutations were in the functional domains. It had been reported that missense *NSD1* mutations were pathogenic only if they occurred in the functional domain (Tatton-Brown et al., 2005).

Although Sotos syndrome was usually associated with prenatal onset overgrowth, 56% of our patients did not have overgrowth at birth (Saugier-Veber et al., 2007; Tatton-Brown et al., 2005). Foster Alison et al. reported that macrocephaly was usually present at any age, but height might normalize in adulthood and the median height in adult female was +1.9 *SD* and male +0.5 *SD* (Foster et al., 2019). Of our two patients who reached adult height, the height SDS of the 19.5-year-old male patient normalized after 10 years of age. Conversely, we detected the height SDS of the 14.3-year-old female patient as +3.25 in her last examination.

The facial features are the most specific diagnostic criterion for Sotos syndrome (Allanson & Cole, 1996; De Boer et al., 2004; Tatton-Brown et al., 2019). In our study, long face, broad forehead, and pointed chin were seen in all patients. We also observed in our patients that long and narrow face in childhood enlarged over time, as reported in the literature (Tatton-Brown et al., 2019).

Consistent with the reported studies, our three patients with a 5q35 microdeletion had lower DQ/IQ values than patients with an intragenic mutation, while other clinical findings were similar in both groups (Saugier-Veber et al., 2007; Tatton-Brown et al., 2005; Tony et al., 2005). We found MRI findings in 61% of the patients; detailed neuroimaging findings of our six patients had already been presented before (Türkmen et al., 2015). Genitourinary (38%) and cardiac system anomalies (38%) were higher in this study than those reported in the literature (De Boer et al., 2004; Saugier-Veber et al., 2007; Tatton-Brown et al., 2005).

Individuals with Sotos syndrome also tend to tumorigenesis (3%), such as sacrococcygeal teratoma, neuroblastoma, and presacral ganglioma in childhood (Tatton-Brown et al., 2019). However, we did not detect any malignancy in our cohort followed up to a median of 6.8 years of age.

4.2.2 | Rahman syndrome

This syndrome caused by *HIST1H1E* mutation is characterized by dysmorphic face, hypotonia, intellectual disability, behavioral disorders and skeletal, cardiac, endocrine, and ectodermal abnormalities (Tatton-Brown et al., 2017). The 1.5 year-old boy, in whom we found known c.441dupC mutation in *HIST1H1E*, had typical facies, camptodactyly, DD and advanced bone age; type 2 diabetes mellitus and hepatosteatosis developed during follow up. The growth pattern of individuals with Rahman syndrome is characterized by a height that is above average in infancy which becomes closer to average over time (Takenouchi et al., 2018). Flex et al. reported that 63% (12/19) of patients had macrocephaly (Flex et al., 2019). Our patient was followed up to adulthood; While his macrocephaly continued, his height had regressed to within normal limits.

4.2.3 | IDDSELD syndrome

A known heterozygous variant in *SETD1B* was found in one of our patients with overgrowth, infantile hypotonia, intellectual disability, and facial dysmorphism. *SETD1B* has not been described among the genes associated with overgrowth syndromes, so far. However, previous studies have reported overgrowth in individuals with de novo microdeletion in the 12q24.3 region encompassing *SETD1B* (Baple et al., 2010; Qiao et al., 2013). It has been reported that 17 of 36 patients with overweight/obesity (17/36) and three with macrocephaly in a cohort with *SETD1B* (Weerts et al., 2021). Macrosomia and macrocephaly persisted in the patient, who was followed up from the infantile period to the age of 11 years. Based on this information, we suggest that *SETD1B* mutations may also cause overgrowth.

4.2.4 | Imagawa-Matsumoto syndrome

To date only 13 patients with monoallelic *SUZ12* variants have been reported in patients with overgrowth, facial dysmorphism, and DD/ID (Cyrus, Cohen, et al., 2019; Imagawa et al., 2017; Imagawa et al., 2018). We identified a novel biallelic variants in the Zn domain of *SUZ12* in two sibs. Although this biallelic variant was considered to be of uncertain significant according to ACMG criteria, it was accepted as causing a disease since it was found to be heterozygous in both parents and located in the zinc finger domain which was responsible for binding PRC2 to DNA and RNA. Cyrus, Cohen, et al. (2019) reported that some heterozygous carriers seemed to be unaffected or mildly affected. In our family severe motor and mental

retardation were detected in the patients, while their parents who were heterozygous carriers were observed to have normal intelligence. The siblings had a round face, micrognatia and full cheeks in their infancy similar to reported patients. However the 7-year-old elder brother had an elongated face, beak-shaped nose, elbow dislocation, and severe contractures in the elbow and knee which were not previously described in the literature (Imagawa et al., 2017, 2018).

4.3 | Syndromes resulting from defects in genes involved in other growth pathways

4.3.1 | *PIK3CA*-related overgrowth spectrum

This spectrum ranges from isolated macrodactyly to generalized overgrowth. *PIK3CA* variants usually occur in the mosaic state, but germline variants have also been reported in 13 patients to date (Rivière et al., 2012; Zollino et al., 2019). In this study, we identified two heterozygous missense variants in *PIK3CA*; One of them was found in blood sample of the P23. The germline variants of *PIK3CA* were reported to be associated with a mild phenotype (Zollino et al., 2019). Our patient had macrocephaly, macrosomia, mild DD and a few minor dysmorphic features. A 9-year-old girl with the same mutation as in our patient, in a mosaic state, presented a more severe cranial and vascular involvement (Rivière et al., 2012). However, the patient in whom we detected somatic mutation had only macrocephaly and capillary malformation.

4.3.2 | Keipert syndrome

The *GPC4* has been mapped to Xq26 and encodes a proteoglycan structurally similar to that of *GPC3*. Further, the coding sequences of *GPC3* and *GPC4* are located closely, with exon 1 of *GPC4* adjacent to the 3-prime end of *GPC3*. Some studies reported that rearrangements (deletion or duplication) in *GPC4* can cause SGBS-like phenotype (Amor et al., 2019; Schirwani et al., 2019; Veugelers et al., 1998; Waterson et al., 2010). We identified two different variants in *GPC4* in two male patients. They had overlapping craniofacial features with SGBS-1, which is caused by *GPC3* mutations and had relative macrocephaly, although one of them had severe growth retardation due to chronic kidney disease.

4.3.3 | Thauvin-Robinet-Faivre syndrome

This syndrome is caused by biallelic mutations in *FIBP*, which encodes an intracellular protein that binds to acidic fibroblast growth factor (aFGF). It is presumed that *FIBP* might be associated with a mitogenic action (Akawi et al., 2016). To date, only four patients (three sibs and an unrelated boy) with a biallelic mutation in *FIBP* have been reported (Akawi et al., 2016; Thauvin-Robinet et al., 2016). We detected a frameshift biallelic variant in *FIBP* in our patient who had overgrowth, mild intellectual disability and facial findings similar to previously reported patients. He was graduated from vocational high school at the age of 19. While macrocephaly was not detected in reported three siblings, our patient had macrocephaly, consistent with the first reported patient. We noticed thick eyebrows in reported patients, similar to our patient, which might be a characteristic feature of the syndrome (Akawi et al., 2016; Thauvin-Robinet et al., 2016).

4.3.4 | IDDCDF syndrome

We identified a biallelic pathogenic variant in *TMEM94* in a boy who was 2.2 year-old with a severe speech delay and facial dysmorphism similar to reported two Turkish patients who had the same mutation (Stephen et al., 2018). *TMEM94* has not been identified among genes associated with OGID syndromes, however, 6 out of 10 patients reported so far have had overgrowth similar to ours (Stephen et al., 2018). Also, *TMEM94* is known for the possible interaction with *FIBP* caused by Thauvin-Robinet-Faivre syndrome (Xu et al., 2014). Therefore, we suggested that the biallelic *TMEM94* mutation could be evaluated among the OGID syndromes. In our patient, who was followed up to the age of 7.7, the height, weight and head circumference SDS progressed to +4.1, +3.7 and +3.3, respectively.

4.3.5 | Cantu syndrome

A known pathogenic monoallelic variant in *ABCC9* was found in a patient with hallmarks features for Cantu syndrome. Cantu is a channelopathy due to pathogenic variants in *ABCC9*, characterized by hypertrichosis, coarse facial features, cardiovascular abnormalities and characteristic skeletal findings. Many of them have macrosomia and macrocephaly, usually present at birth with findings which typically persists throughout life with a developmental delay (63%) (Grange et al., 2019). We identified that unlike previous reports our patient had no DD.

We also compared the patients with Sotos syndrome and other OGID syndromes, the advanced bone age and large hands/feet were more significant in the patients with Sotos syndrome ($p = 0.02$ and 0.001, respectively). The long face, high-arched palate, and pointed chin were also significantly higher in the patients with Sotos syndrome (Table 3). High broad forehead was present in all patients except the P21, P25, and P29. Although the difference was not statistically significant, the mean of height, weight, and head circumference were higher in the group with other OGID syndromes than the patients with Sotos syndrome at birth, while these values were higher in patients with Sotos syndrome at the last examination (Table 3). However, patients with Sotos syndrome had mild DD/ID (DQ/IQ: median 69, range 43–82) while those with other OGID syndromes had moderate (DQ/IQ: median 50, range 30–90).

5 | CONCLUSION

We compared the rate, genetic and clinical characteristics of the overgrowth syndrome types in patients who were followed in a single reference center during 20 years. Molecular diagnosis rate was 88%. CNVs were found in five patients, three of them had 5q35 microdeletion encompassing *NSD1*. 22q13.31 and 9q22.3 microdeletions were detected in two. Seven very rare OGID syndromes were described by WES. Twelve novel mutations were described in genes *NSD1*, *FIBP*, *GPC4*, and *SUZ12*. For the first time, biallelic variants in *SUZ12* were described as the cause of Imagawa-Matsumoto syndrome in this study. We also proposed that a mutation in *SETD1B*, might cause overgrowth. Follow-up findings were evaluated in very rare overgrowth syndromes such as Keipert syndrome, Thauvin-Robinet-Faivre and IDDCDF. While some of our patients with OGID syndrome had facial features such as elongated triangular face, hypertelorism, and prominent chin that overlapped with the Sotos syndrome phenotype, the common finding was forehead prominence in most of the patients. Patients with Sotos syndrome had milder ID/DD than the patients with other OGID syndromes. This study contributed to the literature by expanding and clarifying Sotos and other rare OGID syndrome phenotypes.

AUTHOR CONTRIBUTIONS

Aylin Yüksel Ülker: Conceptualization, methodology, investigation, formal analysis, writing-original draft. **Dilek Uludağ Alkaya:** Conceptualization, methodology, investigation. **Ahmet Okay Çağlayan:** Conceptualization, methodology, molecular analysis. **Esra Usluer:** Conceptualization, methodology, investigation. **Ayça Aykut:** Conceptualization, methodology, investigation. **Ayça Aslanger:** Conceptualization, methodology, molecular analysis. **Mehmet Vural:** Conceptualization, methodology, investigation. **Beyhan Tüysüz:** Conceptualization, methodology, formal analysis, investigation, resources, writing-review and editing, supervision.

ACKNOWLEDGMENTS

The authors would like to thank all patients and their families for participating in this study.

FUNDING INFORMATION

This study was funded by Scientific Research Project Coordination Unit of Istanbul University-Cerrahpasa, with the project number TSA-2020-34,957.

CONFLICT OF INTEREST STATEMENT

The authors declare no conflict no interest.

DATA AVAILABILITY STATEMENT

The data that support the findings of this study are available on request from the corresponding author. The data are not publicly available due to privacy or ethical restrictions.

ORCID

Aylin Yüksel Ülker https://orcid.org/0000-0001-8422-6637
Esra Usluer https://orcid.org/0000-0003-4849-2078
Beyhan Tüysüz https://orcid.org/0000-0002-9620-5021

REFERENCES

Akawi, N., Ben-Salem, S., Lahti, L., Partanen, J., Ali, B. R., & Al-Gazali, L. (2016). A recessive syndrome of intellectual disability, moderate overgrowth, and renal dysplasia predisposing to Wilms tumor is caused by a mutation in FIBP gene. *American Journal of Medical Genetics Part A*, *170*, 2111–2118. https://doi.org/10.1002/ajmg.a.37741

Allanson, J. E., & Cole, T. R. (1996). Sotos syndrome: Evolution of facial phenotype subjective and objective assessment. *American Journal of Medical Genetics*, *65*(1), 13–20. https://doi.org/10.1002/(SICI)1096-8628(19961002)65:1<13::AID-AJMG2>3.0.CO;2-Z

Amor, D. J., Stephenson, S. E. M., Mustapha, M., Mensah, M. A., Ockeloen, C. W., Lee, W. S., Tankard, R. M., Phelan, D. G., Shinawi, M., de Brouwer, A. P. M., Pfundt, R., Dowling, C., Toler, T. L., Sutton, V. R., Agolini, E., Rinelli, M., Capolino, R., Martinelli, D., Zampino, G., … Lockhart, P. J. (2019). Pathogenic variants in GPC4 cause Keipert syndrome. *The American Journal of Human Genetics*, *104*, 914–924. https://doi.org/10.1016/j.ajhg.2019.02.026

Baple, E., Palmer, R., & Hennekam, R. C. M. (2010). A microdeletion at 12q24. 31 can mimic Beckwith-Wiedemann syndrome neonatally. *Molecular Syndromology*, *1*, 42–45. https://doi.org/10.1159/000275671

Baujat, G., Rio, M., Rossignol, S., Sanlaville, D., Lyonnet, S., Merrer, M. L., Munnich, A., Gicquel, C., Colleaux, L., & Cormier-Daire, V. (2005). Clinical and molecular overlap in overgrowth syndromes. *American Journal of Medical Genetics Part C: Seminars in Medical Genetics*, *137*, 4–11. https://doi.org/10.1002/ajmg.c.30060

Brioude, F., Toutain, A., Giabicani, E., Cottereau, E., Cormier-Daire, V., & Netchine, I. (2019). Overgrowth syndromes—Clinical and molecular aspects and tumour risk. *Nature Reviews Endocrinology*, *15*, 299–311. https://doi.org/10.1038/s41574-019-0180-z

Burkardt, D. D., Tatton-Brown, K., Dobyns, W., & Graham, J. M., Jr. (2019). Approach to overgrowth syndromes in the genome era. *American Journal of Medical Genetics Part C: Seminars in Medical Genetics*, *181*, 483–490. https://doi.org/10.1002/ajmg.c.31757

Cyrus, S. S., Cohen, A. S. A., Agbahovbe, R., Avela, K., Yeung, K. S., Chung, B. H. Y., Luk, H., Tkachenko, N., Choufani, S., Weksberg, R., Lopez-Rangel, E., Brown, K., Saenz, M. S., Svihovec, S., McCandless, S. E., Bird, L. M., Garcia, A. G., Gambello, M. J., McWalter, K., … Gibson, W. T. (2019). Rare SUZ12 variants commonly cause an overgrowth phenotype. *American Journal of Medical Genetics Part C: Seminars in Medical Genetics*, *181*, 532–547. https://doi.org/10.1002/ajmg.c.31748

Cyrus, S., Burkardt, D., Weaver, D. D., & Gibson, W. T. (2019). PRC2-complex related dysfunction in overgrowth syndromes: A review of EZH2, EED, and SUZ12 and their syndromic phenotypes. *American Journal of Medical Genetics Part C: Seminars in Medical Genetics*, *181*, 519–531. https://doi.org/10.1002/ajmg.c.31754

De Boer, L., Kant, S. G., Karperien, M., van Beers, L., Tjon, J., Vink, G. R., van Tol, D., Dauwerse, H., le Cessie, S., Beemer, F. A., van der Burgt, I., Hamel, B. C. J., Hennekam, R. C., Kuhnle, U., Mathijssen, I. B., Veenstra-Knol, H. E., Schrander Stumpel, C. T., Breuning, M. H., & Wit, J. M. (2004). Genotype-phenotype correlation in patients suspected of having Sotos syndrome. *Hormone Research in Pædiatrics*, *62*, 197–207. https://doi.org/10.1159/000081063

Edmondson, A. C., & Kalish, J. M. (2015). Overgrowth Syndromes. *Journal of Pediatric Genetics*, *4*, 136–143. https://doi.org/10.1055/s-0035-1564440

Flex, E., Martinelli, S., Van Dijck, A., Ciolfi, A., Cecchetti, S., Coluzzi, E., Pannone, L., Andreoli, C., Radio, F. C., Pizzi, S., Carpentieri, G., Bruselles, A., Catanzaro, G., Pedace, L., Miele, E., Carcarino, E., Ge, X., Chijiwa, C., Lewis, M. E. S., … Tartaglia, M. (2019). Aberrant function of the C-terminal tail of HIST1H1E accelerates cellular senescence and causes premature aging. *The American Journal of Human Genetics*, *105*, 493–508. https://doi.org/10.1016/j.ajhg.2019.07.007

Foster, A., Zachariou, A., Loveday, C., Ashraf, T., Blair, E., Clayton-Smith, J., Dorkins, H., Fryer, A., Gener, B., Goudie, D., Henderson, A., Irving, M., Joss, S., Keeley, V., Lahiri, N., Lynch, S. A., Mansour, S., McCann, E., Morton, J., … Tatton-Brown, K. (2019). The phenotype of Sotos syndrome in adulthood: A review of 44 individuals. *American Journal of Medical Genetics Part C: Seminars in Medical Genetics*, *181*, 502–508. https://doi.org/10.1002/ajmg.c.31738

Grange, D. K., Roessler, H. I., McClenaghan, C., Duran, K., Shields, K., Remedi, M. S., Knoers, N. V. A. M., Lee, J. M., Kirk, E. P., Scurr, I., Smithson, S. F., Singh, G. K., Haelst, M. M., Nichols, C. G., & van Haaften, G. (2019). Cantu syndrome: Findings from 74 patients in the International Cantu Syndrome Registry. *American Journal of Medical Genetics Part C: Seminars in Medical Genetics*, *181*, 658–681. https://doi.org/10.1002/ajmg.c.31753

Imagawa, E., Albuquerque, E. V. A., Isidor, B., Mitsuhashi, S., Mizuguchi, T., Miyatake, S., Takata, A., Miyake, N., Boguszewski, M. C. S., Boguszewski, C. L., Lerario, A. M., Funari, M. A., Jorge, A. A. L., & Matsumoto, N. (2018). Novel SUZ12 mutations in Weaver-like syndrome. *Clinical Genetics*, *94*, 461–466. https://doi.org/10.1111/cge.13415

Imagawa, E., Higashimoto, K., Sakai, Y., Numakura, C., Okamoto, N., Matsunaga, S., Ryo, A., Sato, Y., Sanefuji, M., Ihara, K., Takada, Y., Nishimura, G., Saitsu, H., Mizuguchi, T., Miyatake, S., Nakashima, M., Miyake, N., Soejima, H., & Matsumoto, N. (2017). Mutations in genes encoding polycomb repressive complex 2 subunits cause Weaver syndrome. *Human Mutation*, *38*, 637–648. https://doi.org/10.1002/humu.23200

Kamien, B., Ronan, A., Poke, G., Sinnerbrink, I., Baynam, G., Ward, M., Gibson, W. T., Dudding-Byth, T., & Scott, R. J. (2018). A clinical review of generalized overgrowth syndromes in the era of massively parallel sequencing. *Molecular Syndromology*, *9*, 70–82. https://doi.org/10.1159/000484532

Malan, V., Chevallier, S., Soler, G., Coubes, C., Lacombe, D., Pasquier, L., Soulier, J., Morichon-Delvallez, N., Turleau, C., Munnich, A., Romana, S., Vekemans, M., Cormier-Daire, V., & Colleaux, L. (2010). Array-based comparative genomic hybridization identifies a high frequency of copy number variations in patients with syndromic overgrowth. *European Journal of Human Genetics*, *18*, 227–232. https://doi.org/10.1038/ejhg.2009.162

Moirangthem, A., Mandal, K., Saxena, D., Srivastava, P., Gambhir, P. S., Agrawal, N., Shambhavi, A., Nampoothiri, S., & Phadke, S. R. (2021). Genetic heterogeneity of disorders with overgrowth and intellectual disability: Experience from a center in North India. *American Journal of Medical Genetics Part A*, *185*, 2345–2355. https://doi.org/10.1002/ajmg.a.62241

Muller, E. A., Aradhya, S., Atkin, J. F., Carmany, E. P., Elliott, A. M., Chudley, A. E., Clark, R. D., Everman, D. B., Garner, S., Hall, B. D., Herman, G. E., Kivuva, E., Ramanathan, S., Stevenson, D. A., Stockton, D. W., & Hudgins, L. (2012). Microdeletion 9q22. 3 syndrome includes metopic craniosynostosis, hydrocephalus, macrosomia, and developmental delay. *American Journal of Medical Genetics Part A*, *158*, 391–399. https://doi.org/10.1002/ajmg.a.34216

Nevado, J., García-Miñaúr, S., Palomares-Bralo, M., Vallespín, E., Guillén-Navarro, E., Rosell, J., Bel-Fenellós, C., Mori, M. Á., Milá, M., Campo, M., Barrúz, P., Santos-Simarro, F., Obregón, G., Orellana, C., Pachajoa, H., Tenorio, J. A., Galán, E., Cigudosa, J. C., Moresco, A., … Spanish PMS Working Group. (2022). Variability in Phelan-McDermid syndrome in a cohort of 210 individuals. *Frontiers in Genetics*, *13*, 652454. https://doi.org/10.3389/fgene.2022.652454

Neylon, O. M., Werther, G. A., & Sabin, M. A. (2012). Overgrowth syndromes. *Current Opinion in Pediatrics*, *24*, 505–511. https://doi.org/10.1097/MOP.0b013e3283558995

Qiao, Y., Tyson, C., Hrynchak, M., Lopez-Rangel, E., Hildebrand, J., Martell, S., Fawcett, C., Kasmara, L., Calli, K., Harvard, C., Liu, X., Holden, J. J. A., Lewis, S. M. E., & Rajcan-Separovic, E. (2013). Clinical application of 2.7 M cytogenetics array for CNV detection in subjects with idiopathic autism and/or intellectual disability. *Clinical Genetics*, *83*, 145–154. https://doi.org/10.1111/j.1399-0004.2012.01860.x

Richards, S., Aziz, N., Bale, S., Bick, D., Das, S., Gastier-Foster, J., Grody, W. W., Hegde, M., Lyon, E., Spector, E., Voelkerding, K., Rehm, H. L., & ACMG Laboratory Quality Assurance Committee. (2015). Standards and guidelines for the interpretation of sequence variants: A joint consensus recommendation of the American College of Medical Genetics and Genomics and the Association for Molecular Pathology. *Genetics in Medicine*, *17*, 405–423. https://doi.org/10.1038/gim.2015.30

Rivière, J. B., Mirzaa, G. M., O'Roak, B. J., Beddaoui, M., Alcantara, D., Conway, R. L., St-Onge, J., Schwartzentruber, J. A., Gripp, K. W., Nikkel, S. M., Worthylake, T., Sullivan, C. T., Ward, T. R., Butler, H. E., Kramer, N. A., Albrecht, B., Armour, C. M., Armstrong, L., Caluseriu, O., … Dobyns, W. B. (2012). De novo germline and postzygotic mutations in AKT3, PIK3R2 and PIK3CA cause a spectrum of related megalencephaly syndromes. *Nature Genetics*, *44*, 934–940. https://doi.org/10.1038/ng.2331

Saugier-Veber, P., Bonnet, C., Afenjar, A., Drouin-Garraud, V., Coubes, C., Fehrenbach, S., Holder-Espinasse, M., Roume, J., Malan, V., Portnoi, M. F., Jeanne, N., Baumann, C., Héron, D., David, A., Gérard, M., Bonneau, D., Lacombe, D., Cormier-Daire, V., Billette de Villemeur, T., … Bürglen, L. (2007). Heterogeneity of NSD1 alterations in 116 patients with Sotos syndrome. *Human Mutation*, *28*, 1098–1107. https://doi.org/10.1002/humu.20568

Schirwani, S., Novelli, A., Digilio, M. C., Bourn, D., Wilson, V., Roberts, C., Dallapiccola, B., & Hobson, E. (2019). Duplications of GPC3 and GPC4 genes in symptomatic female carriers of Simpson-Golabi-Behmel syndrome type 1. *European Journal of Medical Genetics*, *62*, 243–247. https://doi.org/10.1016/j.ejmg.2018.07.022

Stephen, J., Maddirevula, S., Nampoothiri, S., Burke, J. D., Herzog, M., Shukla, A., Steindl, K., Eskin, A., Patil, S. J., Joset, P., Lee, H., Garrett, L. J., Yokoyama, T., Balanda, N., Bodine, S. P., Tolman, N. J., Zerfas, P. M., Zheng, A., Ramantani, G., … Malicdan, M. C. V. (2018). Bi-allelic TMEM94 truncating variants are associated with neurodevelopmental delay, congenital heart defects, and distinct facial dysmorphism. *The American Journal of Human Genetics*, *103*, 948–967. https://doi.org/10.1016/j.ajhg.2018.11.001

Türkmen, S., Sahin, S., Koçer, N. A. C. I., Peters, H., Mundlos, S., & Tüysüz, B. (2015). Neuroimaging and clinical characterization of Sotos syndrome. *Genetic Counseling*, *26*, 1–12.

Takenouchi, T., Uehara, T., Kosaki, K., & Mizuno, S. (2018). Growth pattern of Rahman syndrome. *American Journal of Medical Genetics Part A*, *176*, 712–714. https://doi.org/10.1002/ajmg.a.38616

Tatton-Brown, K., Douglas, J., Coleman, K., Baujat, G., Cole, T. R. P., Das, S., Horn, D., Hughes, H. E., Temple, I. K., Faravelli, F., Waggoner, D., Türkmen, S., Cormier-Daire, V., Irrthum, A., Rahman, N., & Childhood Overgrowth Collaboration. (2005). Genotype-phenotype associations in Sotos syndrome: An analysis of 266 individuals with NSD1 aberrations. *The American Journal of Human Genetics*, *77*, 193–204. https://doi.org/10.1086/432082

Tatton-Brown, K., Loveday, C., Yost, S., Clarke, M., Ramsay, E., Zachariou, A., Elliott, A., Wylie, H., Ardissone, A., Rittinger, O., Stewart, F., Temple, I. K., Cole, T., Childhood Overgrowth Collaboration, Mahamdallie, S., Seal, S., Ruark, E., & Rahman, N. (2017). Mutations in epigenetic regulation genes are a major cause of overgrowth with

intellectual disability. *The American Journal of Human Genetics*, *100*, 725–736. https://doi.org/10.1016/j.ajhg.2017.03.010

Tatton-Brown, K., Cole, T. R. P., & Rahman, N. (2019). *Sotos syndrome*. GeneReviews® https://www.ncbi.nlm.nih.gov/books/NBK1479/

Tatton-Brown, K., & Weksberg, R. (2013). Molecular mechanisms of childhood overgrowth. *American Journal of Medical Genetics Part C: Seminars in Medical Genetics*, *163*, 71–75. https://doi.org/10.1002/ajmg.c.31362

Thauvin-Robinet, C., Duplomb-Jego, L., Limoge, F., Picot, D., Masurel, A., Terriat, B., Champilou, C., Minot, D., St-Onge, J., Kuentz, P., Duffourd, Y., Thevenon, J., Rivière, J. B., & Faivre, L. (2016). Homozygous FIBP nonsense variant responsible of syndromic overgrowth, with overgrowth, macrocephaly, retinal coloboma and learning disabilities. *Clinical Genetics*, *89*, e1–e4. https://doi.org/10.1111/cge.12704

Tony, M. T., Edgar, W. H., Ivan, F. L., Daniel, H. C., & Stephen, T. L. (2005). Spectrum of NSD1 gene mutations in southern Chinese patients with Sotos syndrome. *Chinese Medical Journal*, *118*, 1499–1506.

Veugelers, M., Vermeesch, J., Watanabe, K., Yamaguchi, Y., Marynen, P., & David, G. (1998). GPC4, the gene for human K-Glypican, FlanksGPC3on Xq26: Deletion of theGPC3–GPC4Gene cluster in one family with Simpson–Golabi–Behmel syndrome. *Genomics*, *53*, 1–11. https://doi.org/10.1006/geno.1998.5465

Waterson, J., Stockley, T. L., Segal, S., & Golabi, M. (2010). Novel duplication in glypican-4 as an apparent cause of Simpson–Golabi–Behmel syndrome. *American Journal of Medical Genetics Part A*, *152*, 3179–3181. https://doi.org/10.1002/ajmg.a.33450

Weerts, M. J., Lanko, K., Lanko, K., Guzmán-Vega, F. J., Jackson, A., Ramakrishnan, R., Cardona-Londoño, K. J., Peña-Guerra, K. A., van Bever, Y., van Paassen, B. W., Kievit, A., van Slegtenhorst, M., Allen, N. M., Kehoe, C. M., Robinson, H. K., Pang, L., Banu, S. H., Zaman, M., Efthymiou, S., … Barakat, T. S. (2021). Delineating the molecular and phenotypic spectrum of the SETD1B-related syndrome. *Genetics in Medicine*, *23*, 2122–2137. https://doi.org/10.1038/s41436-021-01246-2

Xu, S., Li, X., Gong, Z., Wang, W., Li, Y., Nair, B. C., Piao, H., Yang, K., Wu, G., & Chen, J. (2014). Proteomic analysis of the human cyclin-dependent kinase family reveals a novel CDK5 complex involved in cell growth and migration. *Molecular & Cellular Proteomics*, *13*, 2986–3000. https://doi.org/10.1074/mcp.M113.036699

Yamada, H., Shimura, M., Takahashi, H., Nara, S., Morishima, Y., & Go, S. (2020). A familial case of overgrowth syndrome caused by a 9q22.3 microdeletion in a mother and daughter. *European Journal of Medical Genetics*, *63*, 103872. https://doi.org/10.1016/j.ejmg.2020.103872

Zollino, M., Ranieri, C., Grossi, V., Leoni, C., Lattante, S., Mazzà, D., Simone, C., & Resta, N. (2019). Germline pathogenic variant in PIK3CA leading to symmetrical overgrowth with marked macrocephaly and mild global developmental delay. *Molecular Genetics & Genomic Medicine*, *7*, e845. https://doi.org/10.1002/mgg3.845

SUPPORTING INFORMATION

Additional supporting information can be found online in the Supporting Information section at the end of this article.

How to cite this article: Yüksel Ülker, A., Uludağ Alkaya, D., Çağlayan, A. O., Usluer, E., Aykut, A., Aslanger, A., Vural, M., & Tüysüz, B. (2023). An investigation of the etiology and follow-up findings in 35 children with overgrowth syndromes, including biallelic *SUZ12* variant. *American Journal of Medical Genetics Part A*, *191*A:1530–1545. https://doi.org/10.1002/ajmg.a.63180